The Journal of Experimental Biology 215, 3324-3333

doi:10.1242/jeb.072975

RESEARCH ARTICLE

Symmorphosis and the insect respiratory system: a comparison between flight and hopping muscle

Edward P. Snelling[1,*], Roger S. Seymour[1], Sue Runciman[2], Philip G. D. Matthews[3] and Craig R. White[3]

[1]School of Earth and Environmental Sciences, University of Adelaide, South Australia 5005, Australia, [2]Anatomy and Histology, Flinders University of South Australia, South Australia 5001, Australia and [3]School of Biological Sciences, University of Queensland, St Lucia, Queensland 4072, Australia

*Author for correspondence (edward.snelling@adelaide.edu.au)

SUMMARY

Weibel and Taylor's theory of symmorphosis predicts that the structural components of the respiratory system are quantitatively adjusted to satisfy, but not exceed, an animal's maximum requirement for oxygen. We tested this in the respiratory system of the adult migratory locust *Locusta migratoria* by comparing the aerobic capacity of hopping and flight muscle with the morphology of the oxygen cascade. Maximum oxygen uptake by flight muscle during tethered flight is 967±76 μmol h^{-1} g^{-1} (body mass specific, ±95% confidence interval CI), whereas the hopping muscles consume a maximum of 158±8 μmol h^{-1} g^{-1} during jumping. The 6.1-fold difference in aerobic capacity between the two muscles is matched by a 6.4-fold difference in tracheole lumen volume, which is $3.5\times10^{8}\pm1.2\times10^{8}$ μm^{3} g^{-1} in flight muscle and $5.5\times10^{7}\pm1.8\times10^{7}$ μm^{3} g^{-1} in the hopping muscles, a 6.4-fold difference in tracheole inner cuticle surface area, which is $3.2\times10^{9}\pm1.1\times10^{9}$ μm^{2} g^{-1} in flight muscle and $5.0\times10^{8}\pm1.7\times10^{8}$ μm^{2} g^{-1} in the hopping muscles, and a 6.8-fold difference in tracheole radial diffusing capacity, which is 113±47 μmol kPa^{-1} h^{-1} g^{-1} in flight muscle and 16.7±6.5 μmol kPa^{-1} h^{-1} g^{-1} in the hopping muscles. However, there is little congruence between the 6.1-fold difference in aerobic capacity and the 19.8-fold difference in mitochondrial volume, which is $3.2\times10^{10}\pm3.9\times10^{9}$ μm^{3} g^{-1} in flight muscle and only $1.6\times10^{9}\pm1.4\times10^{8}$ μm^{3} g^{-1} in the hopping muscles. Therefore, symmorphosis is upheld in the design of the tracheal system, but not in relation to the amount of mitochondria, which might be due to other factors operating at the molecular level.

Key words: anatomical diffusing capacity, insect, locust, mitochondria, stereology, symmorphosis, tracheal system.

Received 24 March 2012; Accepted 16 April 2012

INTRODUCTION

Weibel and Taylor's theory of symmorphosis posits that the oxygen delivery steps of the respiratory system are quantitatively adjusted so that no single component limits maximum oxygen flow during strenuous exercise (Weibel et al., 1998; Weibel et al., 1991; Weibel et al., 1992). The theory reasons that natural selection should act to minimise excess capacity along the oxygen cascade because building and maintaining unused respiratory structure is a waste of resources and places unnecessary loads on the body. In support of this, Weibel, Taylor and co-workers showed that the 2.5-fold difference in maximum oxygen consumption rate between 'athletic' and 'non-athletic' mammals (Taylor et al., 1987a) is matched by an equivalent difference in the mitochondrial volume of the locomotory muscles (Hoppeler et al., 1987), the oxygen-carrying capacity of capillaries servicing the locomotory muscles (Conley et al., 1987), and the convective limits of the cardiovascular system (Karas et al., 1987b). However, they also found that the higher aerobic potential of athletic mammals is only partly matched by an increase in pulmonary anatomical diffusing capacity (Weibel et al., 1987a). In fact, mammalian lungs appear to have up to 3-times the diffusing capacity required to saturate blood with oxygen, even during heavy exercise (Karas et al., 1987a). Thus, the economic design principles of symmorphosis are upheld for each step of the mammalian respiratory system, except for the lung, where an excess capacity is evident (Canals et al., 2010; Hsia et al., 1992; Taylor et al., 1987b; Weibel et al., 1991).

However, the respiratory system of mammals and other vertebrates may not offer the best model on which to test for symmorphosis. In particular, the multiple functions of the cardiovascular system make it difficult to establish whether the design is geared towards oxygen delivery or some other function, such as substrate supply, carbon dioxide removal, lactate removal or heat dispersal (Dudley and Gans, 1991; Garland, 1998; Garland and Huey, 1987). It has also been suggested that optimal matching between structural elements in a system becomes increasingly unlikely as the number of elements increases, along with the number of functions performed by each element (Dudley and Gans, 1991). On this basis, the insect respiratory system might offer a more suitable model as oxygen delivery occurs entirely along the tubular branching networks of the tracheal system, which ultimately terminate as small blind-ending tracheoles that function primarily to service the aerobic needs of nearby cells (Snelling et al., 2011b; Wigglesworth, 1983). The structure of the tracheal system is less likely to be constrained by its need to eliminate carbon dioxide, as the high liquid solubility of this gas allows it to diffuse rapidly through the insect's tissues and haemolymph, as well as diffusing laterally across the walls of larger tracheae and air sacs (Schmitz and Perry, 1999; Wigglesworth, 1965). Furthermore, oxygen flux through the insect respiratory system is higher than in any other animal (Casey et al., 1985; Suarez, 2000), and if animals are designed optimally, as symmorphosis suggests, then it should be most evident in species that have experienced strong selective pressure for high aerobic performance (Jones and Lindstedt, 1993).

An allometric assessment of the migratory locust *Locusta migratoria* respiratory system has shown that throughout ontogeny the hopping muscles' aerobic capacity scales in proportion with the total volume, surface area and anatomical diffusing capacity of the tracheoles, and the total volume and inner membrane surface area of the mitochondria (Snelling et al., 2011b). The study therefore provides strong evidence that the insect respiratory system conforms to the economic design principles of symmorphosis. However, the assessment is only half-complete because a non-allometric study, analogous to Weibel, Taylor and colleagues' comparison of athletic *versus* non-athletic mammals, has not yet been undertaken. The challenge is to find either a pair of similar sized insects with vastly different aerobic metabolic ceilings, or better, one insect that utilises different locomotory modes requiring very different energy inputs. In particular, a comparison could be made between highly aerobic flight muscles and less aerobic running or hopping muscles.

The aim of the present study was to assess whether the difference in aerobic capacity between the flight and hopping muscles of the adult migratory locust is matched by a proportional difference in the amount of respiratory structure between the two muscles, as predicted by symmorphosis. The flight muscles contain predominantly fast phasic-type fibres (Kutsch and Usherwood, 1970; Mizisin and Ready, 1986; Wilson and Weis-Fogh, 1962), whereas the hopping muscles contain a mixture of fast phasic-type, slow tonic-type and intermediate-type fibres (Cochrane et al., 1972; Hoyle, 1978). Earlier respirometry revealed that the maximum oxygen consumption rate of adult hopping muscles during jumping exercise averages 158 μmol h^{-1} g^{-1} body mass (Snelling et al., 2011a), whereas the flight muscle consumes a maximum of 967 μmol h^{-1} g^{-1} during tethered-flight exercise (Snelling et al., 2012). According to the principles of symmorphosis, the 6.1-fold difference in aerobic capacity between the hopping and flight muscles should be matched by an equivalent difference in the overall volume, surface area and anatomical diffusing capacity of the tracheoles in the two muscles, and also in the total volume and inner membrane surface area of the mitochondria in the two muscles.

MATERIALS AND METHODS

Animals

Gregarious-phase locusts *L. migratoria* (Linnaeus 1758) were reared at 33±1°C, under a 12 h:12 h light–dark cycle, with *ad libitum* access to seedling wheatgrass and wheat germ, as previously described (Snelling et al., 2011a). Newly emerged adults were identified from the breeding colony and were placed into separate plastic terraria with other adults of similar age. Morphometric analysis of the flight muscles housed within the pterothorax (mesothorax and metathorax) was conducted on adult locusts (N=3 individuals) 2–3 weeks post-final moult, by which time the flight muscles have fully developed (Mizisin and Ready, 1986). Morphometric analysis of the metathoracic femurs (hopping leg femurs) was conducted on adult locusts (N=3 individuals) 3–4 days post-final moult, which is sufficient time for the exoskeleton to stiffen while minimising compression of the tracheal system due to growth (Greenlee and Harrison, 2004; Queathem, 1991). All locusts were fasted 6–10 h prior to tissue fixation consistent with earlier respirometry studies (Snelling et al., 2011a; Snelling et al., 2012).

Specimen preparation

Dissection

The procedure used to dissect and fix locust tissue was modified from methods used in previous electron microscopy studies of insects and spiders (Biserova and Pflüger, 2004; Hartung et al., 2004; Kohnert et al., 2004; Schmitz and Perry, 2002a; Schmitz and Perry, 2002b). The dorsal longitudinal muscle and dorsoventral muscles (tergosternal, tergocoxal, basalar, subalar and tergotrochanteral muscles) constitute almost the entire muscle mass of the pterothorax (Albrecht, 1953; Snodgrass, 1929) and are all recruited for flight (Wilson, 1962). Adults used to obtain morphological data on the flight muscles were initially cold anaesthetised for 20 min in a refrigerator at 4°C, and then weighed to 0.1 mg on an analytical balance (AE163, Mettler, Greifensee, Switzerland). The wings and legs were removed with angled spring scissors, while the head, prothorax and abdomen were removed with a razor. The gut and other organs were withdrawn from the remaining pterothoracic cavity. The left and right sides of the pterothorax were then separated with a razor, and from each half, the dorsal longitudinal muscle was removed, and the dorsoventral muscles of the mesothorax separated from those of the metathorax. Each muscle piece was labelled left or right and by its anatomical name.

The large extensor tibialis muscle and the smaller flexor tibialis muscle constitute the entire muscle mass of the metathoracic femur (Albrecht, 1953; Snodgrass, 1929) and are both recruited during hopping locomotion (Bennet-Clark, 1975; Gabriel, 1985a; Gabriel, 1985b). Adults used to obtain morphological data on the metathoracic femur were cold anaesthetised for 20 min, weighed to 0.1 mg, and then both femurs from each locust were carefully removed with angled spring scissors. A razor was then used to slice each femur along the transverse plane into 12 equal length pieces that were sequentially numbered proximally to distally and labelled left or right.

Fixation and embedding

The fixation and embedding process was performed over 5 consecutive days as detailed in an earlier study (Snelling et al., 2011b), and was identical for flight and hopping muscle. Briefly, immediately following dissection, the tissue pieces were immersed into a chemical fixative solution of 2.5% glutaraldehyde and 2% formaldehyde in 0.2 mol l^{-1} phosphate buffer with pH 7.4. The tissue was then rinsed and placed into a 1% aqueous solution of osmium tetroxide, and then rinsed again and placed into a 2% aqueous solution of uranyl acetate, and then rinsed for a third time before being dehydrated in a 50–100% ethyl alcohol series followed by immersion in pure propylene oxide. Lastly, the tissue was incrementally infiltrated with embedding resin (Durcupan, Fluka, Buchs, Switzerland), placed into individually labelled embedding moulds and covered with pure resin, which was left to polymerise in a 70°C oven for 48 h.

Sampling and analysis

Light microscopy

One pterothorax half and one femur from each locust were randomly selected for light microscopy analysis. Twelve sections were cut along the length of the flight muscles, starting with the anterior end of the dorsal longitudinal muscle, followed by the dorsal end of the mesothoracic dorsoventral muscle, and then the dorsal end of the metathoracic dorsoventral muscle. Twelve sections were also cut proximally to distally along the length of the femur. All sections were 1 μm thick, parallel, transverse, equidistant and cut with 8 mm glass knives and an ultramicrotome (EM UC6, Leica Microsystems, Wetzlar, Germany). The sections were placed onto glass slides, stained with Toluidine Blue, rinsed with distilled water and air dried. Each section was viewed at ×4 magnification under an optical microscope (BX51, Olympus, Hamburg, Germany) and photographed with a mounted digital colour camera (ColorView

Table 1. Number (and magnification) of random electron micrographs taken per adult locust

	Low-magnification tissue images	High-magnification muscle cell images	Mitochondria images	Trachea images
Pterothorax and flight muscle (*N*=3)	36 (×1450)	36 (×4600)	20 (×64,000)	36 (×620–64,000)
Femur and hopping muscle (*N*=3)	44 (×1100)	44 (×4600)	22 (×64,000)	44 (×620–64,000)

III, Soft Imaging System, Olympus), which generated 24 bit, 2576×1932 pixel resolution images. Each section image was imported into a computer graphics program (CorelDRAW 11, Corel Corp., Ottawa, ON, Canada) where a point grid test system was superimposed randomly over the image. The Cavalieri principle, which estimates volume as the product of the structure's summed cross-sectional area and the distance between parallel sections (Cruz-Orive and Weibel, 1990; Howard and Reed, 1998), provided volume estimates for muscle tissue, connective tissue, exoskeleton, class IV tracheae and air sacs (tracheae with a diameter >20 μm), tendon, nerve and haemolymph for each locust. These values were multiplied by two to provide a volume estimate for the whole pterothorax/both femurs per locust. Full details of these measurements and calculations are provided in an earlier study (Snelling et al., 2011b).

Electron microscopy

The remaining pterothorax half and femur from each locust were used for transmission electron microscopy analysis. The sampling scheme randomised section position and angle to produce vertical uniform random sections (Howard and Reed, 1998; Mayhew, 1991). Six sections were cut along the length of the flight muscles and along the length of the femur, in the same order as that used for light microscopy. Each section was 70 nm thick, equidistant and cut with a diamond knife (Diatome, Biel, Switzerland) and ultramicrotome. For the first locust of each group, the first section was cut at a random angle between 0 and 18 deg relative to the vertical plane. For the second locust, the first section was cut at a random angle between 36 and 54 deg, and for the third locust, the first section was cut at a random angle between 72 and 90 deg. For the remaining five sections in each locust, 18 deg was added to the cutting angle with every successive section. This meant that, for each locust, the full range of angles around the vertical plane was randomly sampled.

Sections were placed onto 3 mm copper mesh grids, stained with lead citrate, and viewed with a transmission electron microscope (CM 100, Philips, Eindhoven, The Netherlands) where random 8 bit, 1280×1024 pixel resolution images were captured with a mounted digital camera (MegaView II, Soft Imaging System, Olympus) at appropriate magnifications (Table 1). To obtain unbiased sampling of the flight muscle and femur, the number of random images taken from each section was adjusted relative to the amount of muscle present (Snelling et al., 2011b). All images were exported to CorelDRAW where they were analysed using stereological principles (Cruz-Orive and Weibel, 1990; Howard and Reed, 1998; Mayhew, 1991) appropriate for vertical sections (Baddeley et al., 1986).

Low magnification tissue images (Table 1) were analysed using a point grid test system, which allowed density and volume estimates of muscle, muscle nuclei, extracellular haemolymph, secretory cells, nerve, tendon, lipid droplets, unidentified cells, and tracheal lumen, cuticle, epidermis and nuclei to be made in each locust. Tracheae were categorised into four size classes based on their inner diameter: class I, 0–2 μm (hereafter referred to as tracheoles); class II, 2–5 μm; class III, 5–20 μm; and class IV and air sacs, >20 μm. Whether tracheoles were intracellular or extracellular was also recorded. High magnification images of random muscle cells (Table 1) were also analysed using a point grid test system and this allowed density and volume estimates of mitochondria, myofibril + sarcoplasmic reticulum, and cytosol in each locust. Mitochondria images (Table 1) were analysed using a cycloid arc test system, which provided the surface area-to-volume ratio of the inner and outer mitochondrial membrane from which the total inner and outer membrane surface area was calculated for each locust. Trachea images (Table 1) were also analysed using a cycloid arc test system and the ratio of tracheal inner cuticle surface area-to-lumen volume, and tracheal outer epidermal surface area-to-lumen + cuticle + epidermis volume was calculated for each trachea size class (I, II, III and IV) in each locust. The total inner cuticle and outer epidermal surface areas were then calculated for each trachea size class in each locust. Finally, the cuticle and epidermal thickness was measured from the trachea images (Table 1) and this was used to calculate the harmonic mean barrier thickness of the respective layers for each trachea size class in each locust. The tracheole cuticle and epidermal thickness was also used to calculate their respective volumes given the tracheole lumen volume and assuming a cylindrical shape. A detailed account of the methods used to analyse vertical sections using point grid and cycloid arc test systems, as well as the appropriate calculations, is provided in an earlier study (Snelling et al., 2011b).

The anatomical lateral diffusing capacity for oxygen across the tracheal wall (i.e. lateral conductance) was calculated for each trachea size class (I, II, III and IV) in each locust as a function of inner cuticle surface area, cuticle and epidermal harmonic mean barrier thickness, and Krogh's diffusion coefficients for cuticle (chitin; 3.95×10^{-9} μmol O_2 kPa^{-1} h^{-1} μm^{-1}) and epidermis (rat lung tissue; 6.31×10^{-8} μmol O_2 kPa^{-1} h^{-1} μm^{-1}) corrected to 35°C using Q_{10}=1.1 (Bartels, 1971), consistent with the temperature at which respirometry was performed (Snelling et al., 2011a; Snelling et al., 2012). The sum of the lateral diffusing capacities of each trachea size class provided an overall estimate of the lateral diffusing capacity of the entire tracheal system associated with the flight muscle/both hopping muscles in each locust.

Finally, the anatomical radial diffusing capacity for oxygen out of the tracheoles and into the surrounding muscle (i.e. radial conductance) was determined for the flight muscle/both hopping muscles in each locust according to Krogh's cylinder model for radial diffusion (Kreuzer, 1982; Krogh, 1919; Snelling et al., 2011b). This calculation takes into account the tracheoles' inner cuticular radius, outer cuticular radius, outer epidermal radius, the mean radius of the surrounding muscle serviced by each tracheole, and Krogh's diffusion coefficients for cuticle, epidermis and muscle (frog muscle; 4.16×10^{-8} μmol O_2 kPa^{-1} h^{-1} μm^{-1}) corrected to 35°C (Bartels, 1971). The radial diffusing capacity was calculated only for the tracheoles because this is where almost all oxygen exits the tracheal system and enters the muscle (see Results). Fig. 1 illustrates how the model used to estimate tracheole radial diffusing capacity differs from that used to estimate tracheole lateral diffusing capacity; however, full details of all calculations summarised above are provided in an earlier study (Snelling et al., 2011b). The average time to process each locust from initial fixation to the final quantification of muscle ultrastructure was ~6 weeks, which restricted the study to six individuals.

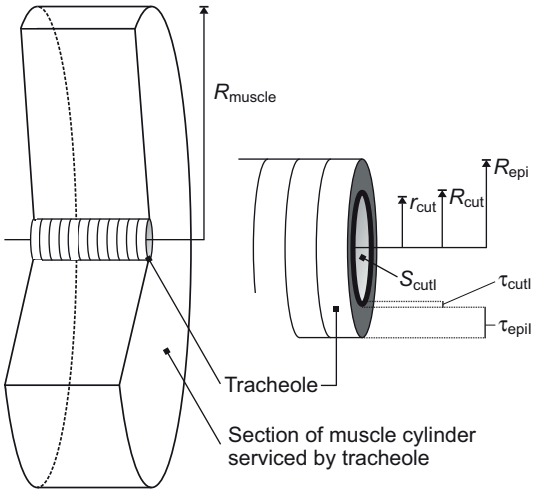

A

$$G_{L,trachI} = 1/\left[\frac{1}{G_{L,cutI}} + \frac{1}{G_{L,epiI}}\right], \text{ where}$$

$$G_{L,cutI} = \frac{S_{cutI}}{\tau_{cutI}} K_{cut},$$

$$G_{L,epiI} = \frac{S_{cutI}}{\tau_{epiI}} K_{epi}.$$

B

$$G_{R,trachI} = 1/\left[\frac{1}{G_{R,cutI}} + \frac{1}{G_{R,epiI}} + \frac{1}{G_{R,muscleI}}\right], \text{ where}$$

$$G_{R,cutI} = K_{cut} / \left[\frac{R_{cut}^2}{2} \ln\frac{R_{cut}}{r_{cut}} - \frac{R_{cut}^2 - r_{cut}^2}{4}\right] V_{cutI},$$

$$G_{R,epiI} = K_{epi} / \left[\frac{R_{epi}^2}{2} \ln\frac{R_{epi}}{r_{cut}} - \frac{R_{epi}^2 - r_{cut}^2}{4}\right] V_{epiI},$$

$$G_{R,muscleI} = K_{muscle} / \left[\frac{R_{muscle}^2}{2} \ln\frac{R_{muscle}}{r_{cut}} - \frac{R_{muscle}^2 - r_{cut}^2}{4}\right] V_{muscle}.$$

Fig. 1. Model used to calculate the total lateral and radial diffusing capacity of class I tracheae (tracheoles) in the flight muscle/both hopping muscles of adult locusts. While the lateral calculation (A) provides a measure of conductance across the tracheole wall only, the radial calculation (B) incorporates the dimensions of the tracheoles, the volume of muscle serviced by the tracheoles, and the dissipation of oxygen molecules further from the tracheole source. Abbreviations; $G_{L,trachI}$ and $G_{R,trachI}$, total lateral and radial diffusing capacity of the tracheoles, respectively; $G_{L,cutI}$, $G_{L,epiI}$, $G_{R,cutI}$, $G_{R,epiI}$ and $G_{R,muscleI}$, lateral diffusing capacity of the tracheole cuticle and epidermal layer, and radial diffusing capacity of the tracheole cuticle, epidermal and surrounding muscle, respectively; K_{cut}, K_{epi} and K_{muscle}, Krogh diffusion coefficients for chitin, rat lung and frog muscle, respectively; r_{cut}, R_{cut}, R_{epi} and R_{muscle}, tracheole inner cuticle, outer cuticle, outer epidermal and serviced muscle radii, respectively; S_{cutI}, total tracheole inner cuticle surface area; τ_{cutI} and τ_{epiI}, tracheole cuticle and epidermal harmonic mean barrier thickness, respectively; V_{cutI}, V_{epiI} and V_{muscle}, total tracheole cuticle, tracheole epidermal and muscle volume, respectively (Snelling et al., 2011b).

All means are presented with 95% confidence intervals (CI). Mean values for maximum oxygen consumption rate, volume, surface area and diffusing capacity are body mass specific, calculated for the whole flight muscle/both hopping muscles per locust. However, mean values for volume density, surface density and thickness are not body mass specific. Statistical significance between two means was tested using unpaired *t*-tests for equal or unequal variance, as appropriate, and when three or more means were compared, an ANOVA was performed (Zar, 1998). Statistical significance between two ratios first required an estimate of variance, which was obtained by calculating the ratios of random combinations of the hopping and flight data before an unpaired *t*-test was performed. The mean ratio calculated from random combinations was generally very close (within 5%) to the ratio calculated by dividing the means of the respective flight and hopping data. All statistical analyses were carried out using GraphPad Prism 5 software (GraphPad Software, La Jolla, CA, USA).

RESULTS

Body mass

Adult locusts used for flight muscle morphometry had a mean body mass of 0.935±0.192 g, and adults used for hopping muscle morphometry had a statistically similar mean body mass of 0.816±0.222 g (*t*-test, P=0.47). There was also no significant difference between the body mass of adult locusts used in the present study and those used in earlier respirometry experiments (ANOVA, P=0.21) (Snelling et al., 2011a; Snelling et al., 2012). Nevertheless, body-mass-specific values are presented (except for volume density, surface density and thickness estimates).

Respirometry

Earlier respirometry studies on adult locusts conducted at 35°C showed that the flight muscle consumes a maximum of 967±76 μmol $O_2\,h^{-1}\,g^{-1}$ body mass during tethered-flight exercise (Snelling et al., 2012), whereas the hopping muscles consume a maximum of 158±8 μmol $O_2\,h^{-1}\,g^{-1}$ during jumping exercise (Snelling et al., 2011a). Therefore, the difference in aerobic capacity between the flight and hopping muscles is 6.1-fold (Table 2).

Morphometry

Muscle volume

Electron micrographs of flight and hopping muscle are presented in Fig. 2. Mean flight muscle volume per locust is $1.6\times10^{11}\pm2.1\times10^{10}$ $\mu m^3\,g^{-1}$ body mass, whereas the combined volume of the two hopping muscles is significantly smaller, $5.2\times10^{10}\pm3.1\times10^{9}$ $\mu m^3\,g^{-1}$ (*t*-test, P<0.05). Assuming a muscle density of 1.06 g ml^{-1} (Mendez and Keys, 1960), the mass of the flight muscle is 0.171±0.022 g g^{-1} body mass (17% of body mass), whereas the combined mass of the two hopping muscles is 0.055±0.003 g g^{-1} (5.5% of body mass). Therefore, the flight muscle's volume (or mass) is 3.1-fold higher than the combined volume (or mass) of the two hopping muscles. However, this falls significantly short of the 6.1-fold difference in the muscles' aerobic capacity (*t*-test, P<0.05).

Tracheal dimensions

The flight muscle's tracheal system volume is 1.8-fold larger than the total volume of the tracheal system associated with both hopping muscles (Table 3). Likewise, the tracheal system's outer epidermal

Table 2. Body-mass-specific maximum oxygen consumption rate

Flight muscle	Hopping muscle	Ratio
967±76	158±8*	6.1-fold

Mean maximum oxygen consumption rate is given in μmol $h^{-1}\,g^{-1}$ body mass (±95% confidence interval, CI) for the flight muscle (N=13) and both hopping muscles (N=23) of adult locusts during heavy exercise at 35°C (Snelling et al., 2011a; Snelling et al., 2012).
*Flight and hopping muscle significantly different (*t*-test; P<0.05).

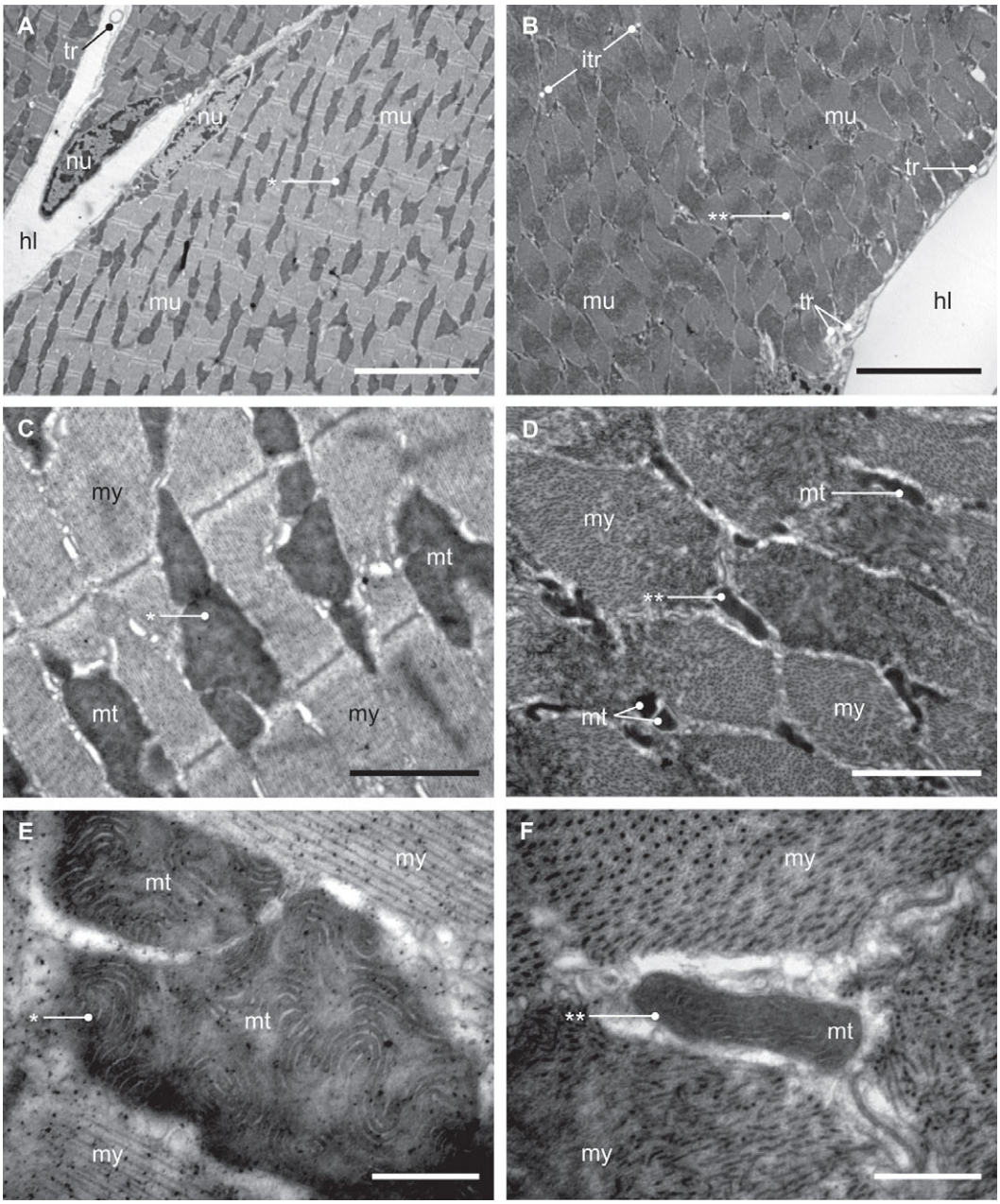

Fig. 2. (A,B) Low magnification electron micrographs (×1950 magnification, scale bar 10 μm) of flight and hopping muscles, respectively. (C,D) Intermediate magnification micrographs (×10,500 magnification, scale bar 2 μm) of flight and hopping muscle fibres, respectively, showing organelle composition and ultrastructure. (E,F) High magnification micrographs (×34,000 magnification, scale bar 0.5 μm) of flight and hopping muscle mitochondria, respectively, showing the difference in size and shape of the organelle in the different muscles, and the distinctive in-folding of the inner membrane (crista). Please note that image orientation changes at each magnification step. Single and double asterisks identify the same single mitochondrion in all micrographs of flight and hopping muscle, respectively. hl, haemolymph; itr, intracellular tracheole; mt, mitochondrion; mu, muscle; my, myofibril; nu, nucleus; tr, tracheole.

surface area and inner cuticle surface area are 2.9- and 3.4-fold larger in the flight muscle compared with both hopping muscles, respectively. Statistical analyses confirm that the total tracheal volume and surface area are significantly larger in the flight muscle (*t*-test, $P<0.05$), but not to the extent that they match the 6.1-fold difference in aerobic capacity (*t*-test, $P<0.05$).

Class I tracheae (tracheoles) constitute approximately 7.5% of tracheal system volume in both hopping and flight muscle (Table 3). The percentage of tracheoles internalised within the fibres of the flight muscle is 37±8%, and in the hopping muscle it is 30±16%, which are statistically indistinguishable (*t*-test, $P=0.47$). Likewise, the volume density of tracheoles in the flight muscle, 0.63±0.07%, is statistically indistinguishable from that of the hopping muscle, 0.67±0.19% (*t*-test, $P=0.73$). However, the volume density of tracheole lumen in the flight muscle is 0.21±0.05%, and this is significantly higher than the 0.10±0.03% recorded in the hopping muscle (*t*-test, $P<0.05$).

The total volume of tracheoles in the flight muscle is 2.9-fold higher than the combined volume of tracheoles in the two hopping muscles (Table 3). Although this is significant (*t*-test, $P<0.05$), it

Table 3. Tracheal surface area and volume

	Flight muscle	Hopping muscle	Ratio
Class I tracheal inner cuticle surface area	$3.2\times10^{9}\pm1.1\times10^{9}$	$5.0\times10^{8}\pm1.7\times10^{8}$*	6.4-fold
Class I tracheal outer epidermal surface area	$4.8\times10^{9}\pm1.1\times10^{9}$	$1.6\times10^{9}\pm3.9\times10^{8}$*	2.9-fold†
Total tracheal inner cuticle surface area	$6.3\times10^{9}\pm1.0\times10^{9}$	$1.9\times10^{9}\pm4.3\times10^{8}$*	3.4-fold†
Total tracheal outer epidermal surface area	$6.9\times10^{9}\pm1.9\times10^{9}$	$2.4\times10^{9}\pm4.5\times10^{8}$*	2.9-fold†
Class I tracheal volume density in muscle – lumen only	0.21±0.05	0.10±0.03*	2.0-fold†
Class I tracheal volume density in muscle	0.63±0.07	0.67±0.19	0.9-fold†
Class I tracheal volume – lumen only	$3.5\times10^{8}\pm1.2\times10^{8}$	$5.5\times10^{7}\pm1.8\times10^{7}$*	6.4-fold
Class I tracheal volume	$1.0\times10^{9}\pm2.3\times10^{8}$	$3.4\times10^{8}\pm8.4\times10^{7}$*	2.9-fold†
Class II tracheal volume	$4.1\times10^{8}\pm4.2\times10^{8}$	$2.4\times10^{8}\pm1.5\times10^{8}$	1.7-fold†
Class III tracheal volume	$1.8\times10^{9}\pm8.7\times10^{8}$	$3.8\times10^{8}\pm1.2\times10^{8}$*	4.8-fold
Class IV tracheal volume	$7.7\times10^{9}\pm1.9\times10^{9}$	$5.0\times10^{9}\pm1.6\times10^{9}$	1.5-fold†
Total tracheal volume	$1.1\times10^{10}\pm9.7\times10^{8}$	$6.0\times10^{9}\pm1.7\times10^{9}$*	1.8-fold†

Mean inner cuticle and outer epidermal surface area ($\mu m^2\,g^{-1}$ body mass, ±95% CI) of class I tracheae (tracheoles), and of the entire tracheal system, associated with the flight muscle (N=3) and both hopping muscles (N=3) of adult locusts. Also shown is the mean volume density (%, ±95% CI) of class I tracheae, and the mean volume ($\mu m^3\,g^{-1}$ body mass, ±95% CI) of class I, II, III and IV tracheae, and of the entire tracheal system, associated with the flight muscle and both hopping muscles.

*Flight and hopping muscle significantly different.

†Ratio significantly different from the 6.1-fold difference in the flight and hopping muscle's aerobic capacity (t-test; P<0.05).

falls significantly short of the 6.1-fold difference in the muscles' aerobic capacity (t-test, P<0.05). However, if the tracheole lumen volume is examined by itself, it is evident that the difference between the two muscles is 6.4-fold (t-test, P<0.05), which is well aligned with the 6.1-fold difference in aerobic capacity (t-test, P=0.66). Likewise, although the 2.9-fold difference in the total surface area of the tracheoles' outer epidermal layer is not matched to aerobic capacity (t-test, P<0.05), the 6.4-fold difference in the total surface area of the inner cuticle is well matched (t-test, P=0.66).

Class II tracheae represent just 4% of tracheal volume in both flight muscle and hopping muscle, and class III tracheae constitute 16% of tracheal volume in flight muscle and 6% in hopping muscle (Table 3). Most of the tracheal volume, therefore, is taken up by large class IV tracheae and air sacs, which represent 70% of the tracheal system's volume in the flight muscle, and 84% in the hopping muscle. However, larger tracheae have thicker walls: the harmonic mean barrier thickness of the cuticle layer increases from approximately 0.032±0.005 μm in class I tracheae to 0.39±0.10 μm in class IV tracheae, and the epidermal layer increases from approximately 0.070±0.028 μm in class I tracheae to 0.46±0.16 μm in class IV tracheae in both hopping and flight muscle (Table 4).

Tracheal diffusing capacity and tracheole service area

The anatomical lateral diffusing capacity (i.e. lateral conductance) of the entire tracheal system in the flight muscle is 385±158 μmol $O_2\,kPa^{-1}\,h^{-1}\,g^{-1}$ body mass at 35°C (Table 5). In comparison, the total tracheal lateral diffusing capacity of the two hopping muscles is significantly less, 82±28 μmol $O_2\,kPa^{-1}\,h^{-1}\,g^{-1}$ (t-test, P<0.05). This 4.7-fold difference is statistically indistinguishable from the 6.1-fold difference in aerobic capacity between the flight and hopping muscle (t-test, P=0.32).

Tracheoles provide approximately 80% of the tracheal system's lateral diffusing capacity for oxygen in both the flight and hopping muscle (Table 5). Therefore, the lateral diffusing capacity of the tracheoles in the flight muscle is 324±144 μmol $O_2\,kPa^{-1}\,h^{-1}\,g^{-1}$ body mass at 35°C, and in both hopping muscles it is once again significantly less, 63±25 μmol $O_2\,kPa^{-1}\,h^{-1}\,g^{-1}$ (t-test, P<0.05). This 5.1-fold difference is also statistically indistinguishable from the 6.1-fold difference in aerobic capacity between the flight and hopping muscle (t-test, P=0.09).

The anatomical radial diffusing capacity (i.e. radial conductance) of the tracheoles is approximately one-third the tracheole lateral diffusing capacity (Table 5). In the flight muscle, it is 113±47 μmol $O_2\,kPa^{-1}\,h^{-1}\,g^{-1}$ body mass at 35°C, and in the hopping muscle it is significantly less, 16.7±6.5 μmol $O_2\,kPa^{-1}\,h^{-1}\,g^{-1}$ (t-test, P<0.05). Once again, this 6.8-fold difference is proportionate to the difference in the muscles' maximum oxygen consumption rate (t-test, P=0.21).

The tracheole radial diffusing capacity is lower than the tracheole lateral diffusing capacity primarily because Krogh's cylinder model for radial diffusion accounts for the extra resistance afforded by the muscle that surrounds each tracheole, through which oxygen must diffuse (Fig. 1). If the muscle and all its tracheoles are simplified to one long tracheole surrounded by a cylinder of muscle, then the mean transverse area of muscle serviced by each tracheole can be calculated as the product of the tracheoles' mean transverse area and the ratio between muscle volume and tracheole volume (Snelling et al., 2011b). According to this, each tracheole in the flight muscle services 119±27 μm^2 of muscle; however, in the hopping muscle the mean tracheole service area is 2-fold larger at approximately 246±70 μm^2 (t-test, P<0.05). Thus, the maximum average distance oxygen must diffuse in flight muscle is 6.1±0.7 μm and in the hopping muscle it is 8.8±1.3 μm.

Table 4. Tracheal harmonic mean barrier thickness

	Flight muscle	Hopping muscle	Ratio
Class I cuticle	0.034±0.005	0.029±0.002	1.2-fold†
Class I epidermis	0.092±0.034	0.047±0.025	2.0-fold†
Class II cuticle	0.061±0.008	0.086±0.021	0.7-fold†
Class II epidermis	0.187±0.038	0.223±0.116	0.8-fold†
Class III cuticle	0.159±0.045	0.143±0.043	1.1-fold†
Class III epidermis	0.273±0.020	0.298±0.096	0.9-fold†
Class IV cuticle	0.315±0.148	0.465±0.043	0.7-fold†
Class IV epidermis	0.463±0.362	0.455±0.064	1.0-fold†

Mean harmonic barrier thickness (μm, ±95% CI) of the inner cuticle and outer epidermal layer of class I, II, III and IV tracheae within the flight muscle (N=3) and hopping muscle (N=3) of adult locusts.

†Ratio significantly different from the 6.1-fold difference in the flight and hopping muscle's aerobic capacity (t-test; P<0.05).

Table 5. Tracheal diffusing capacity and tracheole service area

	Flight muscle	Hopping muscle	Ratio
Service area – class I	119±27	246±70*	0.5-fold†
Radial diffusing capacity – class I	113±47	16.7±6.5*	6.8-fold
Lateral diffusing capacity – class I	324±144	63±25*	5.1-fold
Lateral diffusing capacity – class II	18±29	5.0±4.9	3.6-fold
Lateral diffusing capacity – class III	21±15	5.3±3.8	4.0-fold
Lateral diffusing capacity – class IV	22±13	8.4±4.6	2.6-fold†
Lateral diffusing capacity – all tracheae	385±158	82±28*	4.7-fold

Mean transverse area (μm^2) of muscle serviced by each class I trachea (tracheole), the mean anatomical radial diffusing capacity ($\mu mol\ O_2\ kPa^{-1}\ h^{-1}\ g^{-1}$ body mass, at 35°C, ±95% CI) of the tracheoles, and the mean anatomical lateral diffusing capacity ($\mu mol\ O_2\ kPa^{-1}\ h^{-1}\ g^{-1}$ body mass, at 35°C, ±95% CI) of class I, II, III and IV tracheae, and of the entire tracheal system, within the flight muscle (N=3) and both hopping muscles (N=3) of adult locusts.

*Flight and hopping muscle significantly different.

†Ratio significantly different from the 6.1-fold difference in the flight and hopping muscle's aerobic capacity (t-test; P<0.05).

Mitochondria

Mitochondria occupy 19.7±0.3% of the flight muscle, with a total volume of $3.2\times10^{10}\pm3.9\times10^{9}\ \mu m^3\ g^{-1}$ body mass (Table 6). In comparison, the mitochondrial volume density of the hopping muscle is just 3.1±0.1%, and its total volume in the two hopping muscles is $1.6\times10^{9}\pm1.4\times10^{8}\ \mu m^3\ g^{-1}$. Thus, the 6.4-fold difference in mitochondrial density is statistically indistinguishable from the 6.1-fold difference in aerobic capacity between the flight and hopping muscle (t-test, P=0.60); however, the 19.8-fold difference in total mitochondrial volume is significantly different (t-test, P<0.05).

The mitochondrial inner membrane surface density is approximately $32\ \mu m^2\ \mu m^{-3}$ in both flight muscle and hopping muscle (Table 6). However, the total mitochondrial inner membrane surface area in the flight muscle is $9.9\times10^{11}\pm1.2\times10^{11}\ \mu m^2\ g^{-1}$ body mass, whereas in the hopping muscle it is significantly less, $5.3\times10^{10}\pm5.9\times10^{9}\ \mu m^2\ g^{-1}$ (t-test, P<0.05). This 18.6-fold difference is statistically larger than the 6.1-fold difference in the functional aerobic capacities of the two locomotory muscles (t-test, P<0.05).

DISCUSSION

The locust flight muscle consumes 6.1-fold more oxygen during flight than both hopping muscles consume during jumping exercise (Table 2). However, the flight muscle is only 3.1-times larger than the combined volume of the two hopping muscles, which means that during strenuous exercise, 1 ml of flight muscle consumes around twice the amount of oxygen, per unit time, as 1 ml of hopping muscle. Therefore, if the insect respiratory system conforms to the economic principles of symmorphosis, the total investment made into structures responsible for the delivery (tracheal system) and consumption (mitochondria) of oxygen will be around 6.1-fold higher in the flight muscle compared with the hopping muscles, and thus the density of these respiratory components will be around 2.0-fold higher in the flight muscle than in the hopping muscle (Weibel et al., 1991; Weibel et al., 1992; Weibel et al., 1987b).

Tracheal system and oxygen delivery

The volume of the tracheal system in the flight muscle is around 2-fold larger than that of the hopping muscles (Table 3). Likewise, the inner cuticle and outer epidermal surface of the tracheal system both cover an area that is approximately 3-fold larger in the flight muscle than in the hopping muscles (Table 3). The larger dimensions of the tracheal system associated with the flight muscle is consistent with the greater oxygen requirements for flight, although the magnitude of the difference falls somewhat short of the 6.1-fold predicted by symmorphosis.

Interestingly, much of the tracheal volume can be attributed to large class IV tracheae and air sacs, which function to ventilate the tracheal system (Maina, 1989; Westneat et al., 2003). The absolute volume of class IV tracheae in the flight muscle is just 1.5-fold larger compared with that of both hopping muscles (Table 3). The smaller volume of class IV tracheae in the flight muscle, relative to aerobic capacity, could be due to the efficiency at which the flight muscle's tracheal system is auto-ventilated at wing-stroke frequency (Weis-Fogh, 1964b; Weis-Fogh, 1967). However, one should also consider that the volume of class IV tracheae is likely to decrease with age within the adult life stage as other tissues grow and compress large tracheae (Greenlee and Harrison, 2004).

Table 6. Mitochondria, myofibrils and sarcoplasmic reticulum

	Flight muscle	Hopping muscle	Ratio
Myofibril + sarcoplasmic reticulum volume in muscle	$1.2\times10^{11}\pm1.6\times10^{10}$	$4.9\times10^{10}\pm3.0\times10^{9}$*	2.5-fold†
Mitochondrial volume in muscle	$3.2\times10^{10}\pm3.9\times10^{9}$	$1.6\times10^{9}\pm1.4\times10^{8}$*	19.8-fold†
Myofibril + sarcoplasmic reticulum volume density in muscle	77.2±0.3	94.2±0.2*	0.8-fold†
Mitochondrial volume density in muscle	19.7±0.3	3.1±0.1*	6.4-fold
Mitochondrial inner membrane surface area	$9.9\times10^{11}\pm1.2\times10^{11}$	$5.3\times10^{10}\pm5.9\times10^{9}$*	18.6-fold†
Mitochondrial inner membrane surface density	31.1±2.3	33.0±1.0	0.9-fold†
Mitochondrial outer membrane surface area	$1.6\times10^{11}\pm4.2\times10^{10}$	$2.0\times10^{10}\pm4.1\times10^{9}$*	8.2-fold†
Mitochondrial outer membrane surface density	5.1±1.1	12.4±2.2*	0.4-fold†

Mean volume ($\mu m^3\ g^{-1}$ body mass, ±95% CI) and mean volume density (%, ±95% CI) of the myofibril + sarcoplasmic reticulum complex and mitochondria in the flight muscle (N=3) and both hopping muscles (N=3) of adult locusts. Also shown is the mean mitochondrial inner and outer membrane surface area ($\mu m^2\ g^{-1}$ body mass, ±95% CI) and mean surface density ($\mu m^2\ \mu m^{-3}$ mitochondria, ±95% CI) in the flight and hopping muscle.

*Flight and hopping muscle significantly different.

†Ratio significantly different from the 6.1-fold difference in the flight and hopping muscle's aerobic capacity (t-test; P<0.05).

While large class IV tracheae and air sacs are responsible for ventilation, small terminal class I tracheae (tracheoles) function to transfer oxygen from the tracheal system to the tissue (Hartung et al., 2004; Schmitz and Perry, 1999; Snelling et al., 2011b). It is therefore reasonable to suspect that strong selective pressures should influence the design of the tracheoles such that their functional capacity to deliver oxygen is congruent with the maximum oxygen needs of the tissue they service. The results of the present study seem to confirm this, as a close symmorphotic match exists between the 6.1-fold difference in the aerobic capacity of hopping and flight muscle and the 6.4-fold difference in tracheole lumen volume (Table 3). Physiologically, it is the tracheole lumen volume that is of greatest importance because oxygen delivery along the tracheoles occurs in the gas phase.

Although the tracheole lumen plays a key role in oxygen delivery, the capacity of the tracheal system to deliver oxygen also depends on the dimensions of the tracheole walls, across which oxygen must diffuse. Interestingly, the total tracheole inner cuticle surface area in the flight muscle is 6.4-times larger than in the hopping muscles, and is therefore well matched to the difference in the muscles' aerobic capacity (Table 3). Of course, the thickness of the tracheole walls also influences the rate at which oxygen can diffuse across; however, the harmonic mean barrier thickness of the tracheole cuticle layer in the hopping muscle is statistically indistinguishable from that of the flight muscle, and likewise, the tracheole epidermal thickness is also similar in the two muscles (Table 4). Therefore, the ability of the tracheoles to transfer oxygen from one side of the wall to the other is largely influenced by the inner cuticle surface area, which is factored into the calculation for anatomical lateral diffusing capacity (Fig. 1). Accordingly, the lateral diffusing capacity of tracheoles in the flight muscle is 5.1-fold higher than that of both hopping muscles, which is roughly congruent with the 6.1-fold difference in the muscles' aerobic capacity, as predicted by symmorphosis (Table 5).

However, the tracheoles' lateral diffusing capacity does not account for the extra distance oxygen must travel as it diffuses into the surrounding muscle. It is also relevant that the diffusion of oxygen into the muscle does not occur laterally, but instead follows a radial path, just as oxygen diffuses radially from a capillary source in vertebrate animals. Krogh's cylinder model for radial diffusion (Fig. 1) therefore offers a more appropriate model on which to estimate the true anatomical conductance of the tracheoles (Kreuzer, 1982; Krogh, 1919; Snelling et al., 2011b). According to this model, each tracheole in the hopping muscle services a 246 μm^2 mean cross-sectional area of muscle (radius of 8.8 μm), whereas in the flight muscle, the mean cross-sectional service area is 119 μm^2 (radius of 6.1 μm). Impressively, nearly 50 years ago, Weis-Fogh predicted a 5.4 μm maximum radial diffusion distance for oxygen exiting a 1 μm diameter tracheole in locust flight muscle (Weis-Fogh, 1964a). The 2-fold larger tracheole service area in hopping muscle is congruent with the fact that the hopping muscle's volume-specific aerobic capacity is one-half that of the flight muscle. Therefore, the total anatomical radial diffusing capacity of the tracheoles is 6.8-fold higher in the flight muscle than in the hopping muscles, which is well matched to the 6.1-fold difference in the muscles' functional aerobic capacity (Table 5). Thus, the tracheal system conforms to the economic principles of symmorphosis because it appears that no more tracheole structure exists than is necessary to meet the maximum oxygen requirements of the muscle.

The symmorphotic design of the tracheal system in the flight and hopping muscle of adult locusts adds weight to our earlier allometric assessment, which showed that the increase in the hopping muscles' maximum oxygen consumption rate during juvenile development is associated with a proportional increase in the oxygen delivery capabilities of the tracheal system supplying the hopping muscle (Snelling et al., 2011b). The present study also complements an ontogenetic study on American locusts *Schistocerca americana*, where the convective capacity of large tracheae located between the spiracles and the digestive tract was found to match the metabolic rate of locusts shortly after feeding (Harrison et al., 2005).

Mitochondria as oxygen sinks

While the function of the tracheal system is to deliver oxygen, the function of mitochondria at the end of the respiratory cascade is to use the oxygen to produce ATP. Individual mitochondria tend to be much larger in the flight muscle than in the hopping muscle, but despite this, their inner membrane surface densities are both approximately 32 $\mu m^2 \mu m^{-3}$ (Table 6). Because of this similarity, enzyme concentrations within the mitochondria are also likely to be similar in hopping and flight muscle, as the protein complexes required for oxidative phosphorylation are embedded in the inner membrane (Suarez, 1996).

Given that differences in mitochondrial enzyme concentration are unlikely to contribute towards the 6.1-fold difference in aerobic capacity between the flight and hopping muscle, differences in mitochondrial volume must be considered. The volume density of mitochondria in the hopping muscle is 3.1%, whereas in the flight muscle, mitochondria occupy 19.7% of volume (Table 6). The 6.4-fold higher mitochondrial volume density in the flight muscle, combined with a 3.1-fold larger muscle mass, leads to a total mitochondrial volume that is 19.8-fold higher in the flight muscle compared with the hopping muscle. Clearly, a 19.8-fold higher mitochondrial volume is disproportionate to the 6.1-fold higher aerobic capacity of the flight muscle, and suggests that the flight muscle is over-supplied with mitochondria by a factor of 3-fold. Therefore, the principles of symmorphosis must be rejected at this final step of the oxygen cascade unless an explanation can be found.

The apparent mismatch between the muscle's functional aerobic capacity and its mitochondrial volume is inconsistent with our allometric study on locusts, which showed that the hopping muscle's maximum oxygen consumption rate scales in parallel with its mitochondrial volume throughout juvenile development (Snelling et al., 2011b). It is also inconsistent with several studies on mammals, where aerobic capacity appears to be completely dependent upon the volume of mitochondria in the skeletal muscles (Else and Hulbert, 1985; Hoppeler et al., 1987; Mathieu et al., 1981; Schwerzmann et al., 1989; Weibel et al., 2004).

To further explore this apparent symmorphotic breakdown in the locust respiratory system, it is useful to calculate the aerobic capacity of the mitochondria themselves. Interestingly, 1 ml of locust flight muscle mitochondria can consume a maximum of 12 ml $O_2 min^{-1}$ *in vivo*, which slots predictably between the 7–10 ml $O_2 min^{-1}$ calculated for 1 ml of hummingbird flight muscle mitochondria (Suarez et al., 1991) and the 16–23 ml $O_2 min^{-1}$ calculated for mitochondria in the flight muscle of the bee and blowfly (Suarez, 1996; Suarez et al., 2000). However, the corresponding value for 1 ml of mitochondria in locust hopping muscle is 36 ml $O_2 min^{-1}$ *in vivo*, which is remarkably high relative to the aforementioned estimates, and suggests that other factors might be operating at the molecular level.

This unexpected result demands that all relevant data be closely scrutinised. It seems quite unlikely that either flight or hopping respirometry estimates could be wrong by a factor of 300% given

they correspond well with other published data and given that steps were taken to maximise the work rate of the locomotory muscles through the attachment of weights to exercising locusts (Snelling et al., 2011a; Snelling et al., 2012). It is possible that the adult hopping muscles' aerobic capacity might be slightly over-estimated if ventilatory and/or flight muscles consumed oxygen during jumping exercise; however, ventilatory movements in resting beetles *Psammodes striatus* constitute less than 5% of total energy expenditure (Lighton, 1988), and if the flight muscles did 'twitch' during hopping measurements we showed that any over-estimate is unlikely to exceed 30% (Snelling et al., 2011a). Likewise, it also seems unlikely that Cavalieri calculations of muscle volume could be wrong by 300%. To confirm its accuracy, if the Cavalieri-derived flight muscle volume is converted to a mass estimate assuming a density of 1.06 g ml^{-1} (Mendez and Keys, 1960), it is evident that flight muscles represent around 17% of body mass, which is around the 15–19% estimated for the relative proportion of wet flight muscle tissue in the adult desert locust *S. gregaria*, although this would probably include some fraction of extracellular haemolymph (Fischer and Kutsch, 2000; Weis-Fogh, 1952). Likewise, if hopping muscle volume is converted to mass, we find that together they represent around 5.5% of body mass, which is similar to the 6.4% estimated for adult *S. americana* (Kirkton et al., 2005), after taking into account that ~30% of the femur wet tissue mass is extracellular haemolymph (Hartung et al., 2004; Snelling et al., 2011b). The only other source of potential error is in the calculation of mitochondrial volume density; however, this too seems unlikely given that the 20% mitochondrial density estimated for flight muscle in the present study is consistent with the 21–25% density estimated for flight muscle in the adult vagrant grasshopper *Schistocerca nitens* (Mizisin and Ready, 1986). Likewise, the 3.1% mitochondrial density estimated for hopping muscle in the present study is consistent with the 4.1% density estimated for hopping muscle in adult *S. americana* (Hartung et al., 2004). Given that both respirometry and morphometry data align closely with other reports in the literature, the lack of symmorphotic congruence between aerobic capacity and mitochondrial volume appears to be a genuine phenomenon.

CONCLUSIONS

This study shows that the difference in aerobic capacity between the hopping and flight muscle of adult locusts is matched by a proportional difference in tracheole lumen volume, tracheole inner cuticle surface area, and tracheole lateral and radial diffusing capacity. This suggests that no more tracheal structure exists than is necessary to meet the maximum oxygen needs of the muscle, providing strong evidence that the insect tracheal system conforms to the economic design principles of symmorphosis. This conclusion is in agreement with our earlier ontogenetic allometric assessment of the locust tracheal system (Snelling et al., 2011b).

However, this study also shows that the difference in aerobic capacity between the hopping and flight muscles is not matched by an equivalent difference in the volume of mitochondria in the two muscles. In fact, the flight muscle appears to be over-supplied with mitochondria by a factor of 3-fold. Although our earlier allometric examination found good matching between the volume of mitochondria and functional capacity in the locust hopping muscle throughout development (Snelling et al., 2011b), the results of the present study suggest that symmorphosis should be rejected at this final step of the oxygen cascade unless an explanation can be found. Potentially, factors operating at the molecular level, which cannot easily be quantified using conventional electron microscopy and stereology techniques, are behind this apparent economic breakdown.

Finally, while the present study tests for symmorphosis in the insect respiratory system by searching for simple proportional relationships between functional capacity and structural investment, it would be instructive to complement this research with additional measurements that test for excess capacities by manipulating ambient oxygen partial pressure during locust exercise. If maximum oxygen uptake increases significantly under hyperoxia then it would suggest an over-supply of mitochondria, and if maximum oxygen uptake is maintained under moderate hypoxia then it would suggest an over-investment in the tracheal system. Potentially, some or all of the apparent 3-fold unused aerobic capacity of mitochondria in the locust flight muscle might be functionally realised under an oxygen partial pressure of 63 kPa.

ACKNOWLEDGEMENTS

The authors thank Professor Stephen Simpson and Mr Tim Dodgson from the University of Sydney for technical advice and for providing the founding locust colony. Mr Kerry Gascoigne and Dr Mike Teo of Flinders Microscopy and Ms Ruth Williams and Ms Lyn Waterhouse of Adelaide Microscopy shared their expertise in the field of electron microscopy, which was greatly appreciated. Professor Raul Suarez and two anonymous reviewers provided valuable feedback that led to a much improved manuscript.

FUNDING

This research was supported by the Australian Research Council, project no. DP0879605.

REFERENCES

Albrecht, F. O. (1953). *The Anatomy of the Migratory Locust*. London, UK: Athlone Press.
Baddeley, A. J., Gundersen, H. J. G. and Cruz-Orive, L. M. (1986). Estimation of surface area from vertical sections. *J. Microsc.* **142**, 259-276.
Bartels, H. (1971). Diffusion coefficients and Krogh's diffusion constants. In *Respiration and Circulation* (ed. P. L. Altman and D. S. Dittmer), pp. 21-22. Bethesda, MD: Federation of American Societies for Experimental Biology.
Bennet-Clark, H. C. (1975). The energetics of the jump of the locust *Schistocerca gregaria*. *J. Exp. Biol.* **63**, 53-83.
Biserova, N. M. and Pflüger, H. J. (2004). The ultrastructure of locust pleuroaxillary 'steering' muscles in comparison to other skeletal muscles. *Zoology* **107**, 229-242.
Canals, M., Figueroa, D. P. and Sabat, P. (2010). Symmorphosis in the proximal pathway for oxygen in the leaf-eared mouse *Phyllotis darwini*. *Biol. Res.* **43**, 75-81.
Casey, T. M., May, M. L. and Morgan, K. R. (1985). Flight energetics of euglossine bees in relation to morphology and wing stroke frequency. *J. Exp. Biol.* **116**, 271-289.
Cochrane, D. G., Elder, H. Y. and Usherwood, P. N. R. (1972). Physiology and ultrastructure of phasic and tonic skeletal muscle fibres in the locust, *Schistocerca gregaria*. *J. Cell Sci.* **10**, 419-441.
Conley, K. E., Kayar, S. R., Rosler, K., Hoppeler, H., Weibel, E. R. and Taylor, C. R. (1987). Adaptive variation in the mammalian respiratory system in relation to energetic demand IV: capillaries and their relationship to oxidative capacity. *Respir. Physiol.* **69**, 47-64.
Cruz-Orive, L. M. and Weibel, E. R. (1990). Recent stereological methods for cell biology: a brief survey. *Am. J. Physiol.* **258**, L148-L156.
Dudley, R. and Gans, C. (1991). A critique of symmorphosis and optimality models in physiology. *Physiol. Zool.* **64**, 627-637.
Else, P. L. and Hulbert, A. J. (1985). Mammals: an allometric study of metabolism at tissue and mitochondrial level. *Am. J. Physiol.* **248**, R415-R421.
Fischer, H. and Kutsch, W. (2000). Relationships between body mass, motor output and flight variables during free flight of juvenile and mature adult locusts, *Schistocerca gregaria*. *J. Exp. Biol.* **203**, 2723-2735.
Gabriel, J. M. (1985a). The development of the locust jumping mechanism I: allometric growth and its effect on jumping performance. *J. Exp. Biol.* **118**, 313-326.
Gabriel, J. M. (1985b). The development of the locust jumping mechanism II: energy storage and muscle mechanics. *J. Exp. Biol.* **118**, 327-340.
Garland, T. (1998). Conceptual and methodological issues in testing the predictions of symmorphosis. In *Principles of Animal Design: The Optimization and Symmorphosis Debate* (ed. E. R. Weibel, C. R. Taylor and L. Bolis), pp. 40-47. Cambridge, UK: Cambridge University Press.
Garland, T. and Huey, R. B. (1987). Testing symmorphosis: does structure match functional requirements? *Evolution* **41**, 1404-1409.
Greenlee, K. J. and Harrison, J. F. (2004). Development of respiratory function in the American locust *Schistocerca americana*. II. Within-instar effects. *J. Exp. Biol.* **207**, 509-517.
Harrison, J. F., Lafreniere, J. J. and Greenlee, K. J. (2005). Ontogeny of tracheal dimensions and gas exchange capacities in the grasshopper, *Schistocerca americana*. *Comp. Biochem. Physiol.* **141A**, 372-380.

Hartung, D. K., Kirkton, S. D. and Harrison, J. F. (2004). Ontogeny of tracheal system structure: a light and electron-microscopy study of the metathoracic femur of the American locust, *Schistocerca americana*. *J. Morphol.* **262**, 800-812.
Hoppeler, H., Kayar, S. R., Claasen, H., Uhlmann, E. and Karas, R. H. (1987). Adaptive variation in the mammalian respiratory system in relation to energetic demand III: skeletal muscles setting the demand for oxygen. *Respir. Physiol.* **69**, 27-46.
Howard, C. V. and Reed, M. G. (1998). *Unbiased Stereology: Three Dimensional Measurement in Microscopy.* Oxford, UK: BIOS Scientific Publishers.
Hoyle, G. (1978). Distributions of nerve and muscle fibre types in locust jumping muscle. *J. Exp. Biol.* **73**, 205-233.
Hsia, C. C. W., Herazo, L. F. and Johnson, R. L., Jr (1992). Cardiopulmonary adaptations to pneumonectomy in dogs. I. Maximal exercise performance. *J. Appl. Physiol.* **73**, 362-367.
Jones, J. H. and Lindstedt, S. L. (1993). Limits to maximal performance. *Annu. Rev. Physiol.* **55**, 547-569.
Karas, R. H., Taylor, C. R., Jones, J. H., Lindstedt, S. L., Reeves, R. B. and Weibel, E. R. (1987a). Adaptive variation in the mammalian respiratory system in relation to energetic demand VII: flow of oxygen across the pulmonary gas exchanger. *Respir. Physiol.* **69**, 101-115.
Karas, R. H., Taylor, C. R., Rösler, K. and Hoppeler, H. (1987b). Adaptive variation in the mammalian respiratory system in relation to energetic demand V: limits to oxygen transport by the circulation. *Respir. Physiol.* **69**, 65-79.
Kirkton, S. D., Niska, J. A. and Harrison, J. F. (2005). Ontogenetic effects on aerobic and anaerobic metabolism during jumping in the American locust, *Schistocerca americana*. *J. Exp. Biol.* **208**, 3003-3012.
Kohnert, S., Perry, S. F. and Schmitz, A. (2004). Morphometric analysis of the larval branchial chamber in the dragonfly *Aeshna cyanea* Müller (Insecta, Odonata, Anisoptera). *J. Morphol.* **261**, 81-91.
Kreuzer, F. (1982). Oxygen supply to tissues: the Krogh model and its assumptions. *Experientia* **38**, 1415-1426.
Krogh, A. (1919). The number and distribution of capillaries in muscles with calculations of the oxygen pressure head necessary for supplying the tissue. *J. Physiol.* **52**, 409-415.
Kutsch, W. and Usherwood, P. N. R. (1970). Studies of the innervation and electrical activity of flight muscles in the locust, *Schistocerca gregaria*. *J. Exp. Biol.* **52**, 299-312.
Lighton, J. R. B. (1988). Simultaneous measurement of oxygen uptake and carbon dioxide emission during discontinuous ventilation in the tok-tok beetle, *Psammodes striatus*. *J. Insect Physiol.* **34**, 361-367.
Maina, J. N. (1989). Scanning and transmission electron microscopic study of the tracheal air sac system in a grasshopper *Chrotogonus senegalensis* (Kraus) – Orthoptera: Acrididae: Pyrgomorphinae. *Anat. Rec.* **223**, 393-405.
Mathieu, O., Krauer, R., Hoppeler, H., Gehr, P., Lindstedt, S. L., Alexander, R. M., Taylor, C. R. and Weibel, E. R. (1981). Design of the mammalian respiratory system. VII. Scaling mitochondrial volume in skeletal muscle to body mass. *Respir. Physiol.* **44**, 113-128.
Mayhew, T. M. (1991). The new stereological methods for interpreting functional morphology from slices of cells and organs. *Exp. Physiol.* **76**, 639-665.
Mendez, J. and Keys, A. (1960). Density and composition of mammalian muscle. *Metabolism* **9**, 184-188.
Mizisin, A. P. and Ready, N. E. (1986). Growth and development of flight muscle in the locust (*Schistocerca nitens*, Thunberg). *J. Exp. Zool.* **237**, 45-55.
Queathem, E. (1991). The ontogeny of grasshopper jumping performance. *J. Insect Physiol.* **37**, 129-138.
Schmitz, A. and Perry, S. F. (1999). Stereological determination of tracheal volume and diffusing capacity of the tracheal walls in the stick insect *Carausius morosus* (Phasmatodea, Lonchodidae). *Physiol. Biochem. Zool.* **72**, 205-218.
Schmitz, A. and Perry, S. F. (2002a). Morphometric analysis of the tracheal walls of the harvestmen *Nemastoma lugubre* (Arachnida, Opiliones, Nemastomatidae). *Arthropod Struct. Dev.* **30**, 229-241.
Schmitz, A. and Perry, S. F. (2002b). Respiratory organs in wolf spiders: morphometric analysis of lungs and tracheae in *Pardosa lugubris* (L.) (Arachnida, Araneae, Lycosidae). *Arthropod Struct. Dev.* **31**, 217-230.
Schwerzmann, K., Hoppeler, H., Kayar, S. R. and Weibel, E. R. (1989). Oxidative capacity of muscle and mitochondria: correlation of physiological, biochemical, and morphometric characteristics. *Proc. Natl. Acad. Sci. USA* **86**, 1583-1587.
Snelling, E. P., Seymour, R. S., Matthews, P. G. D., Runciman, S. and White, C. R. (2011a). Scaling of resting and maximum hopping metabolic rate throughout the life cycle of the locust *Locusta migratoria*. *J. Exp. Biol.* **214**, 3218-3224.
Snelling, E. P., Seymour, R. S., Runciman, S., Matthews, P. G. D. and White, C. R. (2011b). Symmorphosis and the insect respiratory system: allometric variation. *J. Exp. Biol.* **214**, 3225-3237.
Snelling, E. P., Seymour, R. S., Matthews, P. G. D. and White, C. R. (2012). Maximum metabolic rate, relative lift, wingbeat frequency and stroke amplitude during tethered flight in the adult locust *Locusta migratoria*. *J. Exp. Biol.* **215**, 3317-3323.
Snodgrass, R. E. (1929). The thoracic mechanism of a grasshopper and its antecedents. *Smithsonian Miscellaneous Collections* **82**, 1-111.
Suarez, R. K. (1996). Upper limits to mass-specific metabolic rates. *Annu. Rev. Physiol.* **58**, 583-605.
Suarez, R. K. (2000). Energy metabolism during insect flight: biochemical design and physiological performance. *Physiol. Biochem. Zool.* **73**, 765-771.
Suarez, R. K., Lighton, J. R. B., Brown, G. S. and Mathieu-Costello, O. (1991). Mitochondrial respiration in hummingbird flight muscles. *Proc. Natl. Acad. Sci. USA* **88**, 4870-4873.
Suarez, R. K., Staples, J. F., Lighton, J. R. B. and Mathieu-Costello, O. (2000). Mitochondrial function in flying honeybees (*Apis mellifera*): respiratory chain enzymes and electron flow from complex III to oxygen. *J. Exp. Biol.* **203**, 905-911.
Taylor, C. R., Karas, R. H., Weibel, E. R. and Hoppeler, H. (1987a). Adaptive variation in the mammalian respiratory system in relation to energetic demand II: reaching the limits to oxygen flow. *Respir. Physiol.* **69**, 7-26.
Taylor, C. R., Weibel, E. R., Karas, R. H. and Hoppeler, H. (1987b). Adaptive variation in the mammalian respiratory system in relation to energetic demand VIII: structural and functional design principles determining the limits to oxidative metabolism. *Respir. Physiol.* **69**, 117-127.
Weibel, E. R., Marques, L. B., Constantinopol, M., Doffey, F., Gehr, P. and Taylor, C. R. (1987a). Adaptive variation in the mammalian respiratory system in relation to energetic demand VI: the pulmonary gas exchanger. *Respir. Physiol.* **69**, 81-100.
Weibel, E. R., Taylor, C. R., Hoppeler, H. and Karas, R. H. (1987b). Adaptive variation in the mammalian respiratory system in relation to energetic demand: I. Introduction to problem and strategy. *Respir. Physiol.* **69**, 1-6.
Weibel, E. R., Taylor, C. R. and Hoppeler, H. (1991). The concept of symmorphosis: a testable hypothesis of structure-function relationship. *Proc. Natl. Acad. Sci. USA* **88**, 10357-10361.
Weibel, E. R., Taylor, C. R. and Hoppeler, H. (1992). Variations in function and design: testing symmorphosis in the respiratory system. *Respir. Physiol.* **87**, 325-348.
Weibel, E. R., Taylor, C. R. and Bolis, L. (1998). *Principles of Animal Design: The Optimization and Symmorphosis Debate*. Cambridge, UK: Cambridge University Press.
Weibel, E. R., Bacigalupe, L. D., Schmitt, B. and Hoppeler, H. (2004). Allometric scaling of maximal metabolic rate in mammals: muscle aerobic capacity as determinant factor. *Respir. Physiol. Neurobiol.* **140**, 115-132.
Weis-Fogh, T. (1952). Fat combustion and metabolic rate of flying locusts. *Philos. Trans. R. Soc. Lond. B* **237**, 1-36.
Weis-Fogh, T. (1964a). Diffusion in insect wing muscle, the most active tissue known. *J. Exp. Biol.* **41**, 229-256.
Weis-Fogh, T. (1964b). Functional design of the tracheal system of flying insects as compared with the avian lung. *J. Exp. Biol.* **41**, 207-227.
Weis-Fogh, T. (1967). Respiration and tracheal ventilation in locusts and other flying insects. *J. Exp. Biol.* **47**, 561-587.
Westneat, M. W., Betz, O., Blob, R. W., Fezzaa, K., Cooper, W. J. and Lee, W. K. (2003). Tracheal respiration in insects visualized with synchrotron x-ray imaging. *Science* **299**, 558-560.
Wigglesworth, V. B. (1965). *The Principles of Insect Physiology.* London, UK: Methuen.
Wigglesworth, V. B. (1983). The physiology of insect tracheoles. *Adv. Insect Physiol.* **17**, 85-148.
Wilson, D. M. (1962). Bifunctional muscles in the thorax of grasshoppers. *J. Exp. Biol.* **39**, 669-677.
Wilson, D. M. and Weis-Fogh, T. (1962). Patterned activity of co-ordinated motor units, studied in flying locusts. *J. Exp. Biol.* **39**, 643-667.
Zar, J. H. (1998). *Biostatistical Analysis.* Englewood Cliffs, NJ: Prentice Hall.